

# Effect of NiO and/or TiO<sub>2</sub> mullite formation and microstructure from gels

M. SALES, J. VILA, J. ALARCÓN

*Departamento de Química Inorgánica. Facultad de Ciencias Químicas, Universidad de Valencia, 46100 Burjasot (Valencia), Spain*

*E-mail: javier.aiareon@uv.es.*

Polymeric and colloidal gels with a constant molar ratio of (Al + Ni and/or Ti)/Si = 3/1 and various (Al/Ni and/or Ti) ratios (up to 21.42 mol% NiO + TiO<sub>2</sub>) were prepared and used to study the effect of the precursor chemical homogeneity on mullite formation processes and the resulting microstructure. Both kinds of gel precursors were preheated at 750 °C for 3 h in order to obtain appropriate gel-derived glasses for further thermal processing. After annealing for several time periods at temperatures between 750 and 1500 °C, differences in crystallization pathways were observed. Polymeric gels crystallized Al–Si and NiAl<sub>2</sub>O<sub>4</sub> spinels from the amorphous form at temperatures in the range between 900 and 1000 °C, depending on the amount of aluminium substitution. Mullite formation was initiated at temperatures between 1100 and 1200 °C, except for the higher substituted 3:2 mullite in which it was produced at 1000 °C. In contrast,  $\gamma$ -Al<sub>2</sub>O<sub>3</sub> and NiAl<sub>2</sub>O<sub>4</sub> spinel were the first crystalline phases identified at 750 °C in specimens from colloidal gels, whereas mullite was formed at temperatures higher than 1200 °C. In specimens with high substitution, mullite was observed at lower temperatures. Although the sequences of reaction from either kind of gel were rather different, mainly at low temperatures (as could be inferred from the chemical homogeneity attained in both gel-derived glasses), the final set of crystalline phases after long annealing at 1400 °C was quite similar. Differences in the microstructure of specimens from either type of gel precursor after annealing at 1400 °C concerned the size of mullite particles and the presence of secondary phases in specimens derived from colloidal precursors. © 1998 Kluwer Academic Publishers

## 1. Introduction

Mullite, nominally 3 Al<sub>2</sub>O<sub>3</sub>·2 SiO<sub>2</sub> is the only stable crystalline compound under normal atmospheric pressure, in the SiO<sub>2</sub>–Al<sub>2</sub>O<sub>3</sub> binary system. Mullite is one of the component phases of traditional ceramics. Moreover, its high strength at high temperature, low thermal expansion and outstanding chemical stability make it an attractive ceramic material for advanced applications. During the last decade, variety of mullite matrix composites have been intensively examined. Thus, zirconia–mullite, cordierite–mullite, alumina–mullite, etc., have given rise to improved mechanical properties [1, 2].

We have recently reported the synthesis and characterization of NiAl<sub>2</sub>O<sub>4</sub> or CoAl<sub>2</sub>O<sub>2</sub> spinel–mullite composites [3–5], using monophasic precursor gels obtained through hydrolysis and polymerization of mixtures of aluminium, silicon and titanium alkoxides and nickel or cobalt chloride. The crystallization sequence of gel-derived glasses previously obtained by preheating gels at 750 °C for 3 h studied by thermal analysis, X-ray diffraction and infrared spectroscopy, was rather different from the path followed by 3:2 stoichiometric mullite prepared using a completely

similar experimental procedure [6]. The microstructure of the final NiAl<sub>2</sub>O<sub>4</sub> or CoAl<sub>2</sub>O<sub>2</sub> spinel–mullite composites revealed the presence of small particles of either spinel dispersed in a mullite matrix. This microstructural feature strongly supports the use of these spinel–mullite composites as ceramic pigmenting systems at high temperature.

Another sol–gel technique which may be used for the preparation of spinel–mullite composites is the so-called colloidal gel, in which a lower level of mixing than for polymeric gel is reached. As has been reported before, the state of mixing of gel precursors prepared by the colloidal gel method is determined by the particle size of the sols; however, the level attained by the polymeric gel can lead to a molecular mixing. This approach has enabled a better understanding of the rather different crystallization pathway in samples of 3:2 stoichiometric mullite obtained by either method of the preparation of the gel precursor, by which a molecular mixing yielded mullite at temperatures above 1000 °C, whereas colloidal specimens crystallized mullite at temperatures higher than 1200 °C [6–8]. However, transformation processes in polymeric systems are very dependent on the chemical

processes from which the gel precursor was obtained [9]. This assumption is clearly evident for 3:2 mullite specimens in which some alumina–silica segregation occurs, mainly brought about by chemical processing conditions. The above heterogeneity gives rise to Al–Si spinel crystallization as the first crystalline phase instead of mullite. Likewise, even though chemical homogeneity was reached during the gel formation process, it should be maintained using further favourable process conditions to prevent silica–alumina segregation and, as a consequence, Al–Si spinel crystallization.

Some previously reported DTA results in substituted 3:2 mullites, in which aluminium was substituted by nickel and/or titanium, prepared according to the method which provides completely homogeneous gels in the  $\text{SiO}_2\text{--Al}_2\text{O}_3$  system [5], indicated the Al–Si spinel formation to be the first crystalline phase at temperatures below 1000 °C, whereas mullite appeared at temperatures in the range between 1100 and 1200 °C. This finding could be interpreted in terms of those reactions and experimental conditions that lead to the segregation of alumina and silica on processing gel precursors. Thus, in principle, this crystallization behaviour indicated that such cations as  $\text{Ni}^{+2}$  and  $\text{Ti}^{+4}$  can play a role as nucleating agents of Al–Si spinel during the thermal processing of gel-derived glasses previously obtained by preheating dried gels at 750 °C for 3 h.

Colloidal or diphasic gels derived from alumina and silica precursors which are present as discrete entities (10–100 nm), also form an Al–Si spinel (or  $\gamma\text{-Al}_2\text{O}_3$ ) which reacts with the silica gel to form orthorhombic mullite at  $\approx 1200$  °C [8]. In fact, the mullite formation temperature changes depending mainly on  $\text{SiO}_2$  and  $\text{Al}_2\text{O}_3$  particle sizes. If the particles used are relatively large, any unreacted portion crystallizes to  $\alpha\text{-Al}_2\text{O}_3$  and cristobalite, which remain up to fairly high temperatures. For this kind of gel precursor, differential thermal analysis shows only a small rounded peak associated with the formation of orthorhombic mullite with  $\approx 60$  mol%  $\text{Al}_2\text{O}_3$  [8]. Likewise, for NiO and/or  $\text{TiO}_2$  substituted 3:2 mullites prepared from colloidal gels, results from differential thermal analysis provide little information on the crystallization pathway of gel precursors. Therefore, in order to follow the reaction sequence of these colloidal gel precursors, X-ray diffraction analysis after thermal treatment at different temperatures is needed. For a better comparison of the reaction sequence of both types of substituted gel, (polymeric and colloidal), the former has been also submitted to the same heating and further analysis by X-ray powder diffraction.

In the present work,  $\text{NiAl}_2\text{O}_4$  spinel–mullite composite powders with several alumina:silica ratios were prepared by the so-called colloidal gel, using boehmite, silicon and titanium colloidal oxides and nickel chloride. An attempt was made to examine and understand the crystallization pathway of colloidal specimens and to compare it with polymeric systems having the same composition. A further objective was to establish evidence of differences in the crystallization rate of mullite for both types of precursor. Finally, differences in the

microstructure of the  $\text{NiAl}_2\text{O}_4$  spinel–mullite composites prepared from both types of gels, were examined.

## 2. Experimental procedure

### 2.1. Preparation of gel samples

Gels with compositions  $3(\text{Al}_{2-2x}\text{Ni}_x\text{Ti}_x\text{O}_3)\cdot 2\text{SiO}_2$  with  $x = 0.025, 0.050$  and  $0.200$ , (samples A, B and C, respectively) were prepared from both polymeric and colloidal precursors, denoted PG and CG, respectively. Likewise, gels with nominal compositions  $3(\text{Al}_{2-x}\text{M}_x\text{O}_3)\cdot 2\text{SiO}_2$  with  $\text{M} = \text{Ni}, \text{Ti}$  and  $x = 0.05$  (samples D and E, respectively), were also prepared by both sol–gel methods. Both PG and CG gels with compositions  $3\text{Al}_2\text{O}_3\cdot 2\text{SiO}_2$  (PG3:2 and CG3:2, respectively) were also prepared and processed in the same way in order to compare the obtained results with those from the substituted specimens. The nominal compositions prepared are summarized in Table I. It should be noted that, except for composition C, all the other tried compositions have  $\text{Al}_2\text{O}_3\cdot 2\text{SiO}_2$  molar ratios in the range from 2.6:2 to 6.3:2 which was claimed previously by Cameron as the boundaries for a continuous solid solution range on the basis of numerous mullites prepared by a variety of methods [10].

PG gels were prepared using, as starting chemicals, tetraethylorthosilicate (TEOS,  $\text{Si}(\text{OC}_2\text{H}_5)_4$ ), aluminium tri-sec-butylate ( $\text{Al}(\text{OC}_4\text{H}_9)_3$ ) and titanium isopropylate ( $\text{Ti}(\text{OC}_3\text{H}_7)_4$ ), all from Merck and Co., and nickel chloride (Fluka), using a procedure previously reported by us [5]. Stoichiometric amounts of aluminium and titanium alkoxides were dissolved in 2-propanol (2-PrOH) by refluxing under a nitrogen atmosphere and added to a prehydrolysed TEOS solution which contained the required amount of nickel chloride. A 1:2 molar ratio of TEOS:H<sub>2</sub>O was used in prehydrolysis which was performed at 40 °C for 20 h. The resultant mixture with a molar ratio TEOS/EtOH = 1/30 was refluxed at 70 °C for 5 d yielding either a green or a colourless gel in nickel- or titanium containing samples, respectively.

Colloidal gels (CG) were prepared by mixing clear boehmite hydrosol, titanium and silicon colloidal oxides and nickel chloride. Boehmite hydrosol was made from acid-peptized  $\text{AlOOH}$ , previously precipitated by hydrolysing aluminium tri-sec-butylate in an excess of water at 70 °C, by adding 1 M  $\text{HNO}_3$  dropwise while

TABLE I Nominal compositions of prepared samples

Sample	Oxide content (mol %) <sup>a</sup>			
	$\text{Al}_2\text{O}_3$	NiO	$\text{TiO}_2$	$\text{SiO}_2$
A	57.63 (69.36)	1.48 (1.31)	1.48 (1.39)	39.41 (27.94)
B	55.34 (66.96)	2.91 (2.58)	2.91 (2.76)	38.84 (27.70)
C	42.86 (53.48)	10.71 (9.79)	10.71 (10.47)	35.72 (26.26)
D	57.63 (69.42)	2.96 (2.61)		39.41 (27.97)
E	57.63 (69.29)		2.96 (2.79)	39.41 (27.92)
3:2	60.00 (71.29)			40.00 (28.21)

<sup>a</sup>The nominal compositions in wt % are given in parentheses.

stirring [11]. Monodispersed, spheroidal titanium oxide was also prepared by the controlled hydrolysis of diluted solutions of titanium isopropylate in isopropanol by mixing with diluted solutions of water in the same solvent [12]. Colloidal silica was a powder that could be easily dispersed in deionized water and it was used as-received from the supplier (Aerosil 200, Degussa AG, Frankfurt, Germany).

The preparation of colloidal gels began with the dissolution of  $\text{NiCl}_2 \cdot 6\text{H}_2\text{O}$  in deionized water (100 ml  $\text{H}_2\text{O}$  per 5 g end product). To this vigorously stirred solution at  $70^\circ\text{C}$ , all the remaining materials were added: colloidal  $\text{SiO}_2$ , boehmite and titanium oxide. After a few minutes, a stable suspension ( $\text{pH} = 2$ ) was obtained to which a solution of ammonium hydroxide was added dropwise until gelation occurred ( $\text{pH} = 5\text{--}6$ ).

All gels (PG and CG) were first slowly dried for several weeks in beakers sealed with a perforated plastic foil for and then dried in an oven at  $120^\circ\text{C}$ . In order to obtain a gel-derived glass, dried samples were preheated at  $750^\circ\text{C}$  for 3 h obtaining beige-coloured gel-derived glasses for all samples except for sample E, which was white in colour. Glass powders were calcined at temperatures in the range between  $900\text{--}1500^\circ\text{C}$  for several periods.

## 2.2. Characterization of samples

The chemical and structural evolution of the dried gels and crystalline specimens were examined using several techniques.

The infrared absorption spectra were measured in the range  $2000\text{--}400\text{ cm}^{-1}$  using the KBr pellet method (on an apparatus model 882 made by Perkin-Elmer). The products were diluted (1%) in dried potassium bromide.

Differential thermal analyses were carried out in air with  $\alpha\text{-Al}_2\text{O}_3$  liners, using a heating rate of  $10^\circ\text{C min}^{-1}$  (with an equipment model 1700 made by Perkin-Elmer). Finely powdered alumina was used as reference substance.

X-ray diffraction analysis was performed using a graphite monochromated  $\text{CuK}_\alpha$  radiation (using an apparatus model D-500, made by Siemens). The diffractometer had two  $1^\circ$  divergence slits, a  $1^\circ$  scatter slit, and a  $0.05^\circ$  receiving slit.

The microstructure of the as-prepared and thermally treated samples was examined by scanning electron microscopy working at  $20\text{--}30\text{ kV}$  and field emission scanning electron microscopy at  $5\text{--}10\text{ kV}$  (with equipment models S-2500 and S-4100, respectively, made by Hitachi). To check the quality of the observation, some of the samples were etched with a diluted HF solution for 10 s, and subsequently washed with  $\text{H}_2\text{O}$ . All specimens were coated with gold in an ion-beam coater.

The energy-dispersive X-ray analysis was performed using a scanning electron microscope (model JSM-6300, made by Jeol) operated at  $20\text{ kV}$ . This instrument is equipped with an energy dispersive X-ray spectrometer (model Pentafet, made by Oxford Instruments). Specimens were mounted in a polymer resin and polished with progressively finer SiC papers.

Before acquiring the X-ray spectra samples were carbon coated.

UV-vis spectra of the specimens were measured using the diffuse reflectance technique (with an instrument model Lambda 9, made by Perkin-Elmer).

## 3. Results and discussion

### 3.1. Gel structure

IR spectra of both types of dried gels PG and CG are shown in Fig. 1. As can be observed, the main difference between them is the presence of bands associated with Si-O-Al bonds in gels prepared by the PG technique. These bands, appearing at  $1020$  and  $875\text{ cm}^{-1}$ , indicate the formation of a aluminosilicate network [13, 14]. For dried CG, however, bands associated with either colloidal silica and boehmite are detected [15]. Thus, bands appearing at around  $1115$ ,  $876$ ,  $565$  and  $475\text{ cm}^{-1}$  and the shoulder at  $1215\text{ cm}^{-1}$  are all associated with colloidal silica. The strong intensity of the band at  $475\text{ cm}^{-1}$  should be noted. On the other hand, bands at  $1070$ ,  $750$ ,  $705$  and  $640\text{ cm}^{-1}$  are all related to colloidal boehmite.

Differences in the structure of both kinds of gel must give rise to a different sequence of reaction with the thermal treatment for gels. Thus, in principle, the higher the level of mixing the higher is the reactivity, and therefore mullite formation in PG specimens should be faster.

### 3.2. Crystallization path of the gels

DTA heating curves for PG gels preheated at  $750^\circ\text{C}$  exhibit at least three exothermic effects [5]. The first one, centred in the range between  $972$  and  $889^\circ\text{C}$ , is associated with crystallization of Al-Si spinel and the other two, between  $1100$  and  $1200^\circ\text{C}$ , to mullite formation. For samples with the highest amount of  $\text{Ni}^{+2}$  and  $\text{Ti}^{+4}$ , the thermal effects associated with the crystallization of mullite are very weak and two further effects are associated with rutile and cristobalite, respectively. In contrast, no clear exothermic effects are observed for colloidal gels. Instead, a very broad exothermic effect occurs over a wide region from about  $700\text{--}1250^\circ\text{C}$ . This fact is in agreement with previously reported results in diphasic 3:2 mullites [8].

A summary of the crystalline phases observed by X-ray powder diffraction for polymeric and colloidal gels heated under nonisothermal conditions to various temperatures, is given in Tables II and III, respectively. As can be seen, the reaction sequence is rather different at low temperature, although the final set is quite similar, at least with respect to the nature and amount of the main crystalline phases.

X-ray powder diffraction patterns for PGB and PGD substituted gels, with compositions  $3(\text{Al}_{1.90}\text{Ti}_{0.05}\text{Ni}_{0.05}\text{O}_3) \cdot 2\text{SiO}_2$  and  $3(\text{Al}_{1.95}\text{Ni}_{0.05}\text{O}_3) \cdot 2\text{SiO}_2$ , respectively (chosen as representative samples), annealed for 8 h at several temperatures are shown in Fig. 2. The evolution of the PG-substituted gel-derived glasses, in samples having different bulk compositions, as a consequence of performing annealing treatments at increasing temperatures between

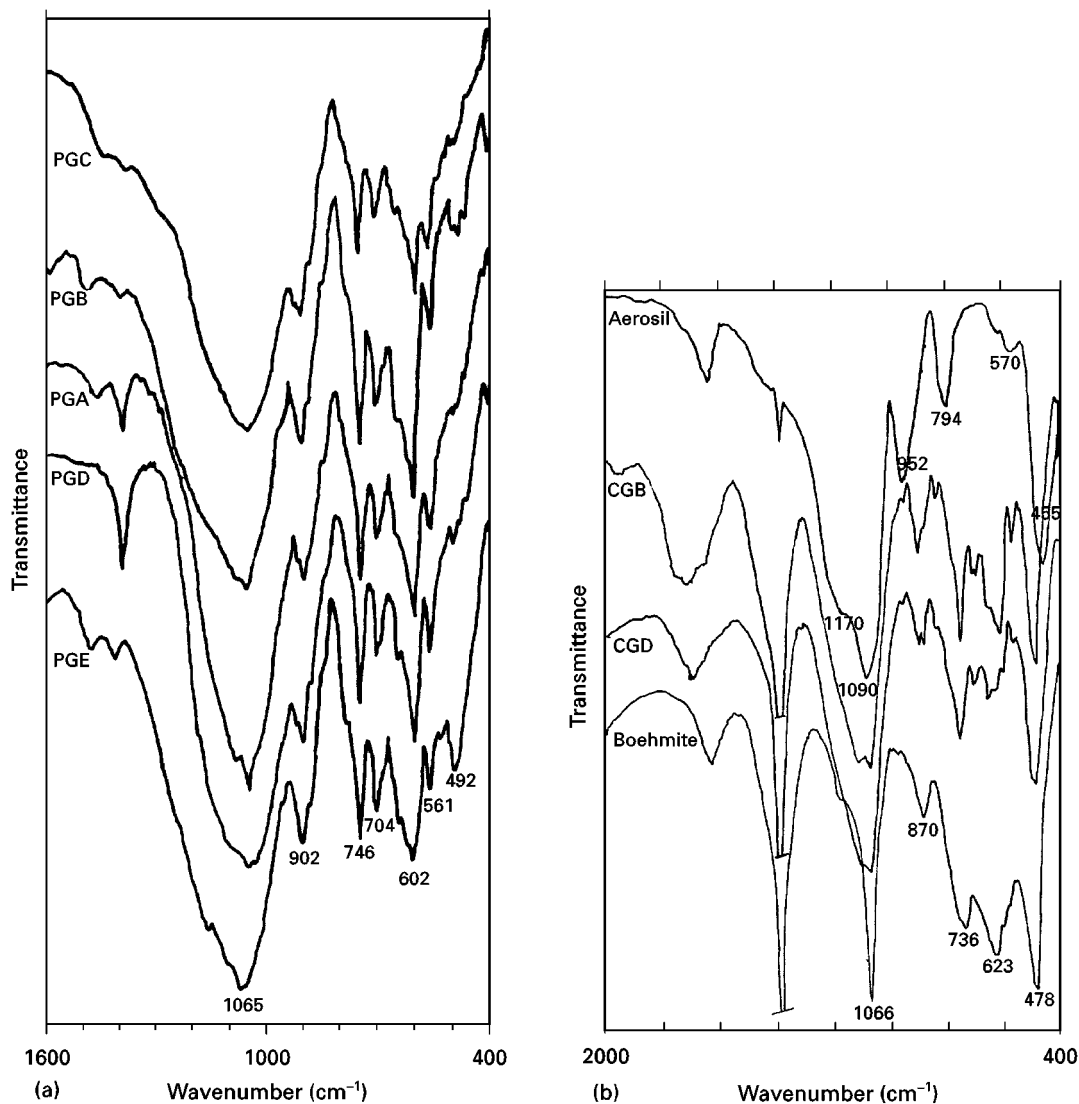


Figure 1 IR spectra of dried gels: (a) polymeric, (b) colloidal.

TABLE II Evolution of crystalline phases in nickel and/or titanium polymeric gels (PG)

Sample	750 °C/3 h	1000 °C/8 h <sup>a</sup>	1100 °C/8 h	1200 °C/8 h <sup>a</sup>	1400 °C/8 h <sup>a</sup>	1400 °C/96 h <sup>b</sup>
A	Amorphous	Al-Si spinel (Ni-Al spinel) + amorphous	Mullite + NiAl <sub>2</sub> O <sub>4</sub> + amorphous	Mullite + NiAl <sub>2</sub> O <sub>4</sub> (traces)	Mullite + NiAl <sub>2</sub> O <sub>4</sub> (traces)	Mullite + NiAl <sub>2</sub> O <sub>4</sub> (traces)
B	Amorphous	Al-Si spinel (Ni-Al spinel) + amorphous	Mullite + NiAl <sub>2</sub> O <sub>4</sub> + amorphous	Mullite + NiAl <sub>2</sub> O <sub>4</sub>	Mullite + NiAl <sub>2</sub> O <sub>4</sub>	Mullite + NiAl <sub>2</sub> O <sub>4</sub> (little)
C	Amorphous	Al-Si spinel (Ni-Al spinel) + Mullite + amorphous	Mullite + NiAl <sub>2</sub> O <sub>4</sub> + Rutile + amorphous	Mullite + NiAl <sub>2</sub> O <sub>4</sub> + Rutile + cristobalite	Mullite + NiAl <sub>2</sub> O <sub>4</sub> + Rutile + cristobalite	Mullite + NiAl <sub>2</sub> O <sub>4</sub> + Al <sub>2</sub> TiO <sub>5</sub>
D	Amorphous	Amorphous + Al-Si spinel (Ni-Al spinel)	Amorphous + Mullite + NiAl <sub>2</sub> O <sub>4</sub>	Mullite + NiAl <sub>2</sub> O <sub>4</sub> + amorphous	Mullite + NiAl <sub>2</sub> O <sub>4</sub>	Mullite + NiAl <sub>2</sub> O <sub>4</sub>
E	Amorphous	Amorphous + Al-Si spinel	Mullite + amorphous	Mullite + amorphous	Mullite	Mullite
3:2	Amorphous	Mullite + amorphous	Mullite + amorphous	Mullite + amorphous	Mullite	Mullite

<sup>a</sup> Only 3 h for 3:2

<sup>b</sup> 1500 °C/30 min for 3:2.

TABLE III Evolution of crystalline phases in Ni/Ti colloidal gels (CG)

Sample	750 °C/3 h	1000 °C/8 h <sup>a</sup>	1200 °C/8 h <sup>a</sup>	1300 °C/8 h <sup>a</sup>	1400 °C/8 h <sup>a</sup>	1400 °C/96 h <sup>b</sup>
A	Amorphous + NiAl <sub>2</sub> O <sub>4</sub> + γ-Al <sub>2</sub> O <sub>3</sub> (traces)	Amorphous + NiAl <sub>2</sub> O <sub>4</sub> + γ-Al <sub>2</sub> O <sub>3</sub> (traces)	Amorphous + cristobalite + corundum + rutile + NiAl <sub>2</sub> O <sub>4</sub> (traces)	Mullite + corundum + cristobalite + NiAl <sub>2</sub> O <sub>4</sub> (traces)	Mullite + corundum + NiAl <sub>2</sub> O <sub>4</sub> (traces)	Mullite + NiAl <sub>2</sub> O <sub>4</sub> (traces)
B	Amorphous + NiAl <sub>2</sub> O <sub>4</sub> + γ-Al <sub>2</sub> O <sub>3</sub>	Amorphous + NiAl <sub>2</sub> O <sub>4</sub> + γ-Al <sub>2</sub> O <sub>3</sub> + anatase	Amorphous + NiAl <sub>2</sub> O <sub>4</sub> + γ-Al <sub>2</sub> O <sub>3</sub> + anatase	Mullite + corundum + NiAl <sub>2</sub> O <sub>4</sub> + rutile	Mullite + corundum + NiAl <sub>2</sub> O <sub>4</sub> + rutile	Mullite + NiAl <sub>2</sub> O <sub>4</sub>
C	Amorphous + anatase + NiAl <sub>2</sub> O <sub>4</sub> + γ-Al <sub>2</sub> O <sub>3</sub>	Amorphous + Anatase + NiAl <sub>2</sub> O <sub>4</sub> + γ-Al <sub>2</sub> O <sub>3</sub>	Rutile + NiAl <sub>2</sub> O <sub>4</sub> + mullite + corundum	Mullite + Rutile + NiAl <sub>2</sub> O <sub>4</sub> + cristobalite	Mullite + NiAl <sub>2</sub> O <sub>4</sub> + rutile + cristobalite	Mullite + NiAl <sub>2</sub> O <sub>4</sub> + rutile + Al <sub>2</sub> TiO <sub>5</sub>
D	Amorphous + NiAl <sub>2</sub> O <sub>4</sub> + γ-Al <sub>2</sub> O <sub>3</sub>	Amorphous + NiAl <sub>2</sub> O <sub>4</sub> + γ-Al <sub>2</sub> O <sub>3</sub>	Amorphous + corundum + NiAl <sub>2</sub> O <sub>4</sub> + γ-Al <sub>2</sub> O <sub>3</sub>	Cristobalite + corundum + mullite + NiAl <sub>2</sub> O <sub>4</sub>	Cristobalite + corundum + mullite + NiAl <sub>2</sub> O <sub>4</sub>	Mullite + NiAl <sub>2</sub> O <sub>4</sub> + corundum (traces)
E	Amorphous + γ-Al <sub>2</sub> O <sub>3</sub> (traces)	Amorphous + γ-Al <sub>2</sub> O <sub>3</sub> + anatase	Cristobalite + mullite + corundum + rutile	Cristobalite + mullite + corundum + rutile	Mullite + corundum + cristobalite + rutile (traces)	Mullite + corundum (traces) + rutile (traces)
3:2	Amorphous + γ-Al <sub>2</sub> O <sub>3</sub> (traces)	Amorphous + γ-Al <sub>2</sub> O <sub>3</sub> + δ-Al <sub>2</sub> O <sub>3</sub>	Mullite + cristobalite + θ-Al <sub>2</sub> O <sub>3</sub> + δ-Al <sub>2</sub> O <sub>3</sub> + amorphous	Mullite + cristobalite + corundum	Mullite + corundum + cristobalite	Mullite + corundum + cristobalite

<sup>a</sup> Only 3 h for 3:2

<sup>b</sup> Only 72 h for 3:2.

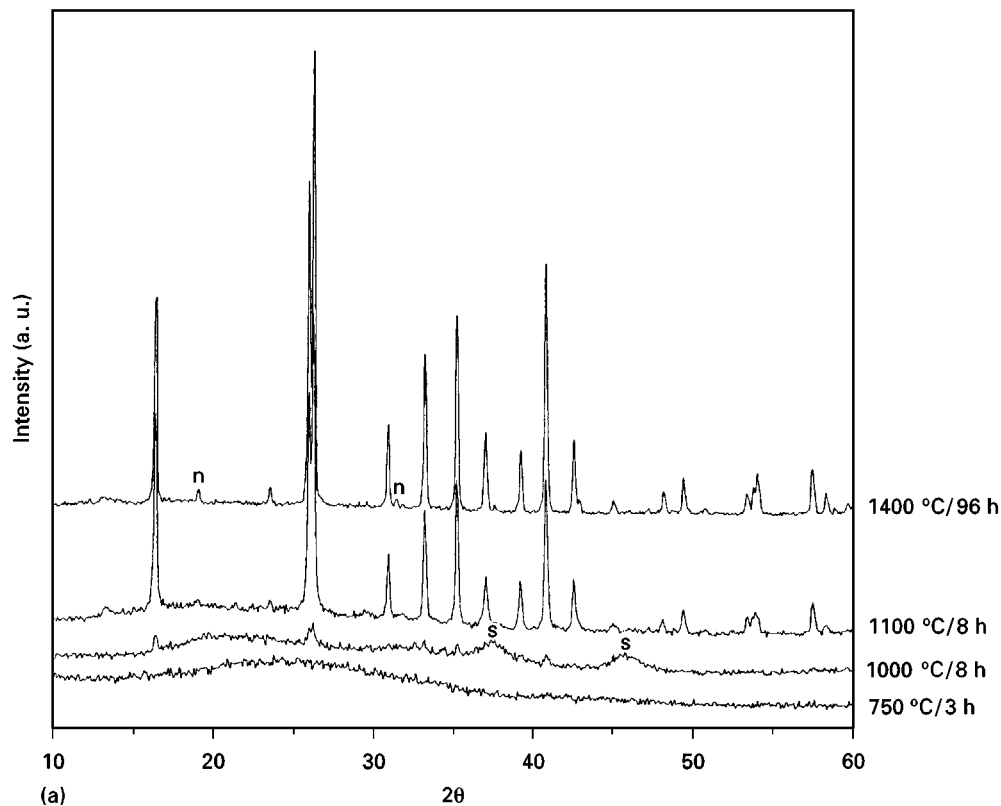


Figure 2 X-ray powder diffraction patterns of polymeric gels heated at several temperatures: (a) PGB, (b) PGD. n, NiAl<sub>2</sub>O<sub>4</sub>; s, Al-Si spinel.

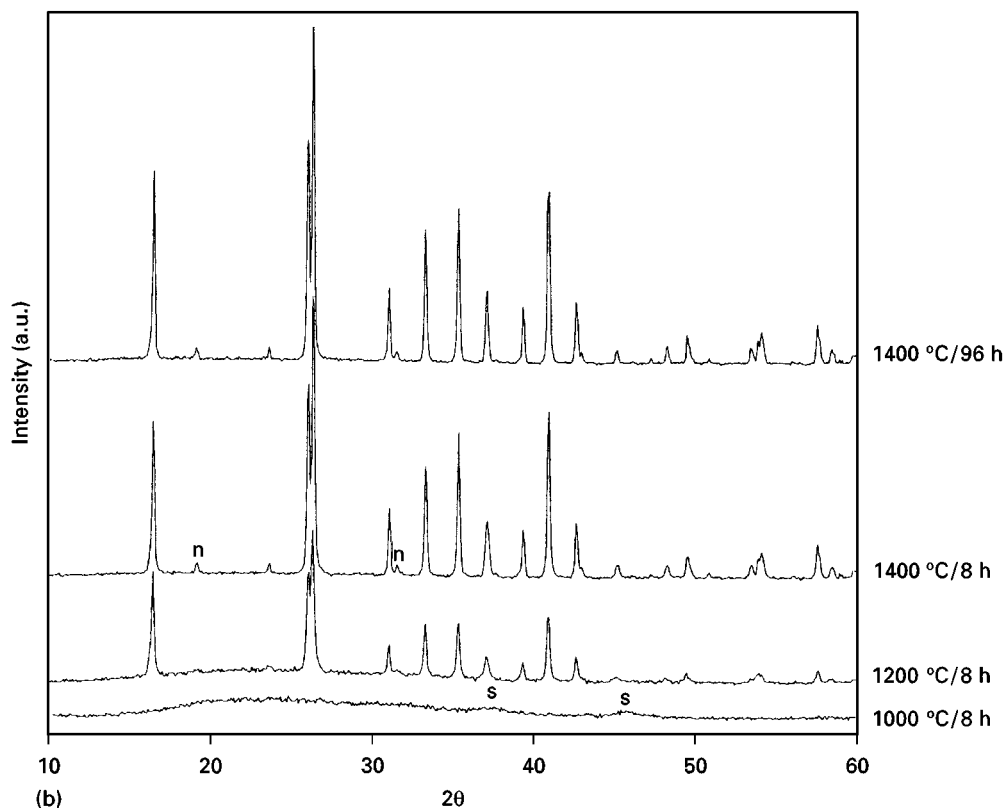


Figure 2 (Continued).

1000 and 1400 °C, can be summarized as follows: (a) the gel derived glasses are amorphous to X-rays until heated at temperatures around 1000 °C; (b) nickel-containing specimens at 1000 °C show crystallization of Al/Si and NiAl<sub>2</sub>O<sub>4</sub> spinels; (c) on increasing the temperature, well-crystallized mullite as well as NiAl<sub>2</sub>O<sub>4</sub> are observed at 1100 °C; (d) only slight differences are observed in the amount of crystalline phases on raising the temperature up to 1400 °C.

The sample PGC (the greater substituted sample) displays some differences in the crystallization path. Thus mullite appears at 1000 °C together with Al/Si and NiAl<sub>2</sub>O<sub>4</sub> spinels. Rutile and cristobalite are also detected at 1100 and 1200 °C, respectively. Both phases are present until 1400 °C but with long annealing they disappear and Al<sub>2</sub>TiO<sub>5</sub> is formed, as shown in Fig. 3.

The CG-substituted gel-derived glasses exhibit radically different behaviour from PG of the same stoichiometry on heating. X-ray powder diffraction patterns with the same nominal compositions as the PG polymeric gels, showed in Fig. 2, are displayed in Fig. 4. NiAl<sub>2</sub>O<sub>4</sub> starts to form below 750 °C for all compositions except for sample CGE in which only  $\gamma$ -Al<sub>2</sub>O<sub>3</sub> is detected. Anatase or rutile, cristobalite and corundum crystallization precedes mullite formation when the gels are heated, confirming the fact that the three discrete phases are reacting independently up to 1200 °C. Mullite formation is initiated at about 1300 °C for all samples except for sample CGC which is observed at 1200 °C. In addition to mullite and NiAl<sub>2</sub>O<sub>4</sub> no other phases are detected in samples

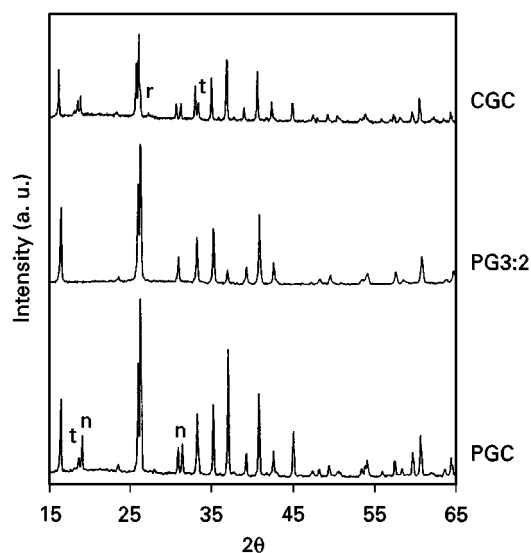


Figure 3 X-ray powder diffraction patterns of the gels PGC, CGC and PG3:2 heated at 1400 °C for 96 h. *r*, rutile; *t*, Al<sub>2</sub>TiO<sub>5</sub>; *n*, NiAl<sub>2</sub>O<sub>4</sub>.

CGA and CGB annealed for a long time at 1400 °C. However, for samples CGD and CGE, corundum and/or rutile are also detected. Al<sub>2</sub>TiO<sub>5</sub> is also observed after long annealing of sample CGC at 1400 °C (Fig. 3). As indicated above, for the same composition in the PG series (sample PGC), Al<sub>2</sub>TiO<sub>5</sub> was also detected.

On comparing crystallization pathways for both PG and CG Ni<sup>+2</sup>-containing compositions, the first

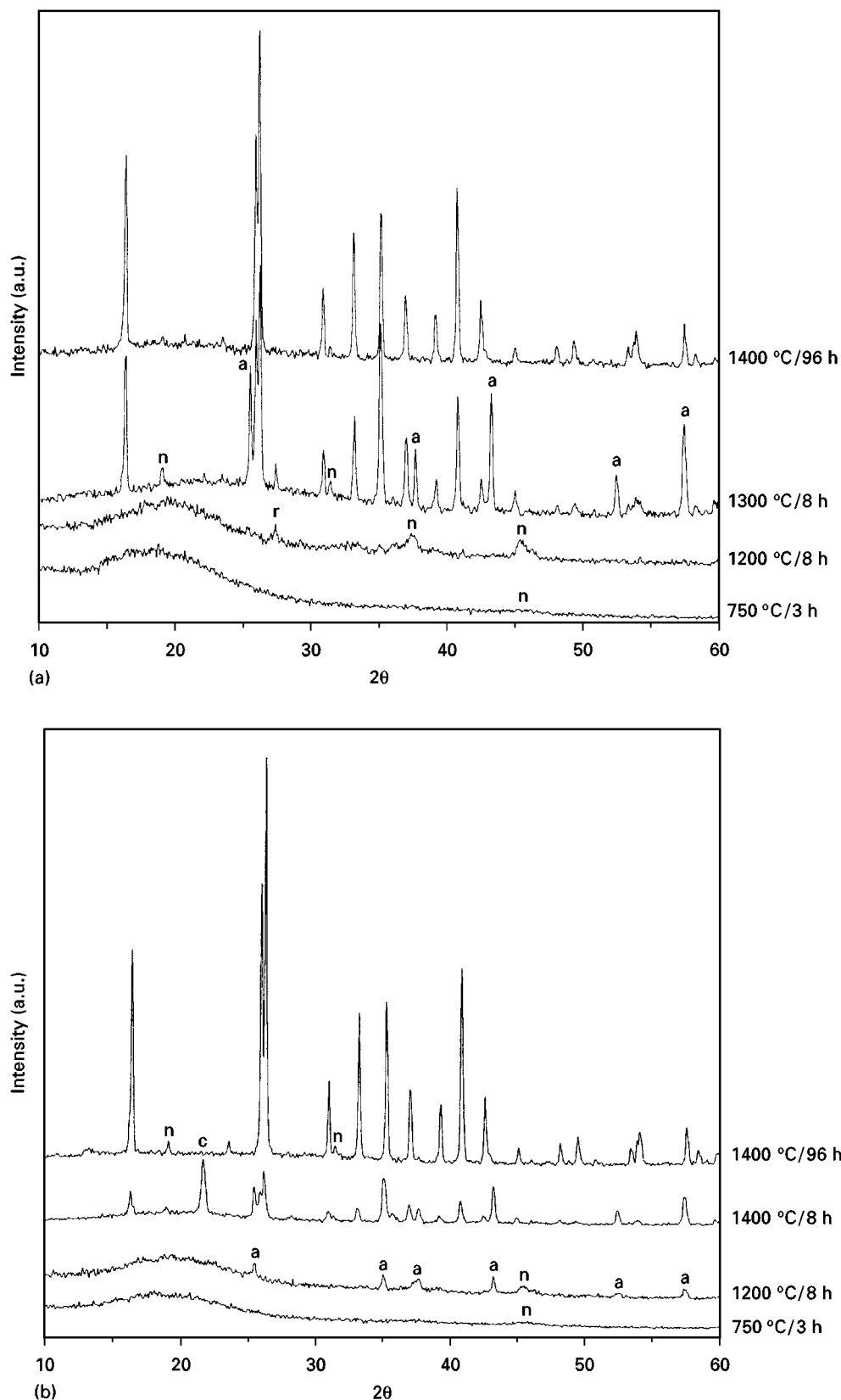


Figure 4 X-ray powder diffraction patterns of colloidal gels heated at several temperatures: (a) CGB, (b) CGD. *a*,  $\alpha$ - $\text{Al}_2\text{O}_3$ ; *r*, rutile; *n*,  $\text{NiAl}_2\text{O}_4$ ; *c*, cristobalite.

difference is the crystallization of  $\text{NiAl}_2\text{O}_4$  at low temperatures in CG specimens. In Fig. 5 shows the UV-Vis spectra of gels PGD and CGD (chosen as representative  $\text{Ni}^{+2}$ -containing samples) heated at 750 °C for 3 h. The spectrum of sample PGD displays a band at around 450 nm which has been attributed to

octahedrally coordinated  $\text{Ni}^{+2}$  [5]. On the other hand, the spectrum of sample CGD closely fits that obtained for  $\text{NiAl}_2\text{O}_4$ . These results are in accordance with those obtained from X-ray powder diffraction experiments (Tables II and III). Thus, the former sample is amorphous while the latter displays the

presence of  $\text{NiAl}_2\text{O}_4$  and/or  $\gamma\text{-Al}_2\text{O}_3$ . Results previously obtained by us have proved the formation of  $\text{NiAl}_2\text{O}_4$  spinel by gelling mixtures of colloidal boehmite solutions and nickel chloride and further heating

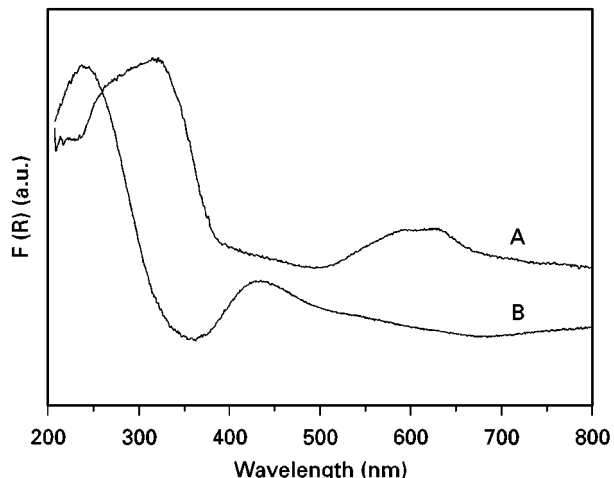


Figure 5 UV-Vis spectra of samples fired at 750 °C for 3 h: (a) CGD, (b) PGD.

at 700 °C [16]. Al-Si spinel, however, could be formed together with  $\text{NiAl}_2\text{O}_4$  its detection is difficult because, at this low temperature, crystallization is rather poor and both spinels present similar patterns due to their similarity in both structure at lattice parameters. In any case, as has been reported in the literature for undoped mullite diphasic gels, the formation of Al-Si spinel is detected at temperatures higher than 1300 °C or not detected at all [17, 18]. Therefore, it can be assumed that the formation of Al-Si spinel in our  $\text{Ni}^{+2}$ -containing CG compositions in the first stage of the reaction, i.e. at 750 °C, can be neglected. Obviously, upon heating, the boehmite transforms to  $\gamma\text{-Al}_2\text{O}_3$  at low temperatures, but it reacts with NiO to form  $\text{NiAl}_2\text{O}_4$ .

The reaction sequence for PG specimens is different, confirming the previously reported crystallization path from DTA studies [5]. In this case, the formation of Al-Si spinel is associated with the first exothermic effect detected by DTA, at temperatures around 1000 °C and further formation of  $\text{NiAl}_2\text{O}_4$  is evident after a slight increase of either temperature or holding

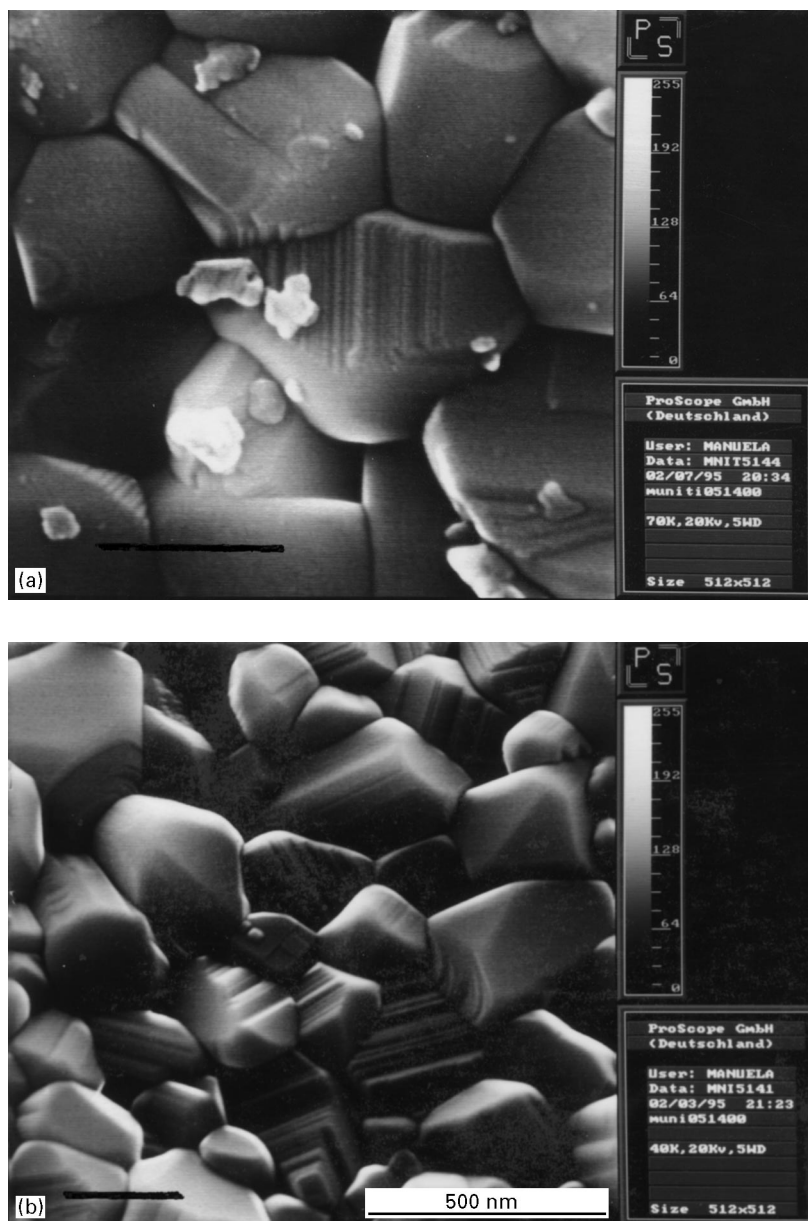


Figure 6 Scanning electron micrographs of polymeric gels heat treated at 1400 °C/96 h: (a) PGB, (b) PGD.



time. The possibility of an epitaxial growth mechanism of  $\text{NiAl}_2\text{O}_4$  on to Al-Si spinel has been suggested.

Some remarks are needed on the mullite formation in both types of gel. In either PG3:2 and CG3:2, i.e. unsubstituted 3:2 specimens, crystalline mullite is formed at 1000 and 1200 °C, respectively. Some small amounts of cristobalite and corundum, however, are still detected for CG3:2 heated at 1400 °C for around 100 h. These results are in accordance with previously reported results [9]. The observed difference in crystallization temperature of mullite for specimens in both series of PG- and CG-substituted gels is also around 200 °C. The crystallization mechanism in either series must be rather different due to the level of mixing, i.e. chemical homogeneity, reached in each one of them. Thus, it was reported that mullite formation from stoichiometric polymeric gels, i.e. single-phase gels, appears to be a nucleation-controlled reaction which differs from the kinetics of mullite formation of stoichiometric and non-stoichiometric diphasic gels

which follows a rapid nucleation and a diffusion-controlled growth process [20–22].

As can be noted, mullite formation in substituted PG gels takes place at higher temperatures than in unsubstituted 3:2. This may be understood by considering the nucleating role played by  $\text{Ti}^{+4}$  and/or  $\text{Ni}^{+2}$  in aluminosilicate gel-derived glasses [5]. Thus, small amounts of  $\text{Ti}^{+4}$  and/or  $\text{Ni}^{+2}$  in two-sep thermally processed PG-substituted gels, provoke some loss of chemical homogeneity, i.e. segregation of alumina and silica in the processing, which favours the formation of Al-Si spinel as the first crystalline phase. The ability of the spinel to forestall mullite formation in the molecular gel has been reported by Huling and Hessing [9].

Mullite formation temperatures in substituted CG gels are quite similar to those reported for unsubstituted gels. Li and Thomson [20] claimed that mullite formation is initiated around 1300 °C in a wide range of compositions in the  $\text{SiO}_2\text{-Al}_2\text{O}_3$  system.



Figure 7 Scanning electron micrographs of colloidal gels heat treated at 1400 °C/96 h: (a) CGB, (b) CGD.

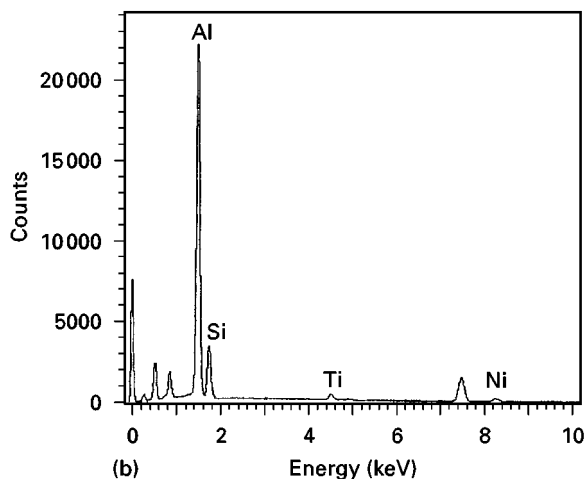
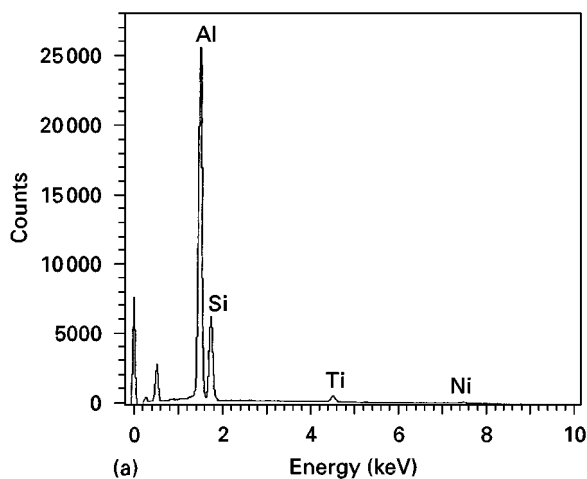
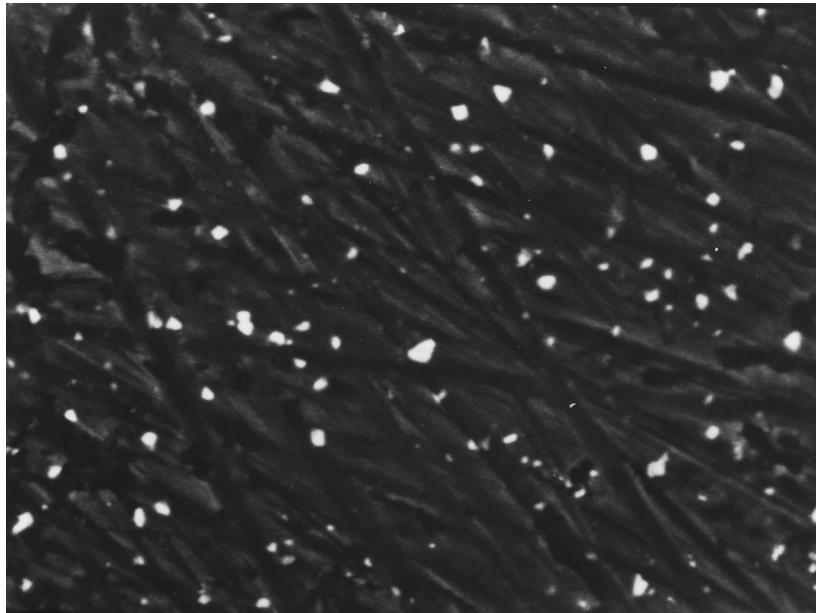


Figure 8 Back-scattered electron micrograph of sample PGB heated at 1400°C/96 h and EDX spectra of (a) dark and (b) light areas.

Therefore, a similar mechanism of reaction controlled by diffusion, can be inferred. For colloidal specimens, mullite conversion is almost complete at 1400°C according to the XRD measurements. There are some residues of unreacted materials at the higher temperatures. This fact can be understood by taking into

account that further reaction requires diffusion of the alumina trapped within the mullite grains, which it is known to be very slow.

Thus, both kinds of polymeric and colloidal gels preheated at 750°C lead to NiAl<sub>2</sub>O<sub>4</sub> spinel–mullite composites, but differences are referred to the reaction sequence mainly at lower temperatures. These behaviours are in agreement with previously reported results obtained for mullite single phase and diphasic gels [20, 21, 23].

### 3.3. Microstructure

Scanning electron micrographs of both series of specimens annealed for long times at 1400°C are shown in Figs 6 and 7. As can be seen from pictures there are no strong differences between both series of prepared samples. From the observed microstructures as a function of composition in the PG series [5], it was inferred that the larger the amount of substitution, that is the SiO<sub>2</sub>-richer the compositions, the larger are the amount and size of prismatic mullite particles. This feature was in accordance with reported results in which elongated prismatic particles were obtained for compositions richer in silica than the stoichiometric 3:2, which suggested crystal growth via a low viscous liquid phase [20, 24]. The only clear difference between both series of samples is related to the size of mullite particles. The larger sizes are seen for CG specimens, whereas generally the sizes for PG are smaller, independently of the composition.

In all cases, where only mullite solid solution and NiAl<sub>2</sub>O<sub>4</sub> crystalline phases are detected, small areas of different contrast in secondary electron images are also observed. The differences are increased with backscattered electron images as shown in Figs 8 and 9. This observation clearly indicates areas of different composition. After analysing both dark and light areas in samples PGB, heated at 1400°C/96 h, by EDX spectroscopy (Fig. 8a and b), the lighter areas may be associated with NiAl<sub>2</sub>O<sub>4</sub> spinel particles. So, these specimens heated at 1400°C for several hours

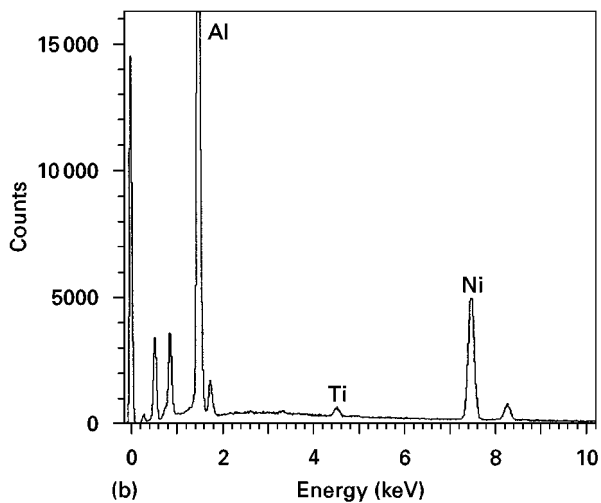
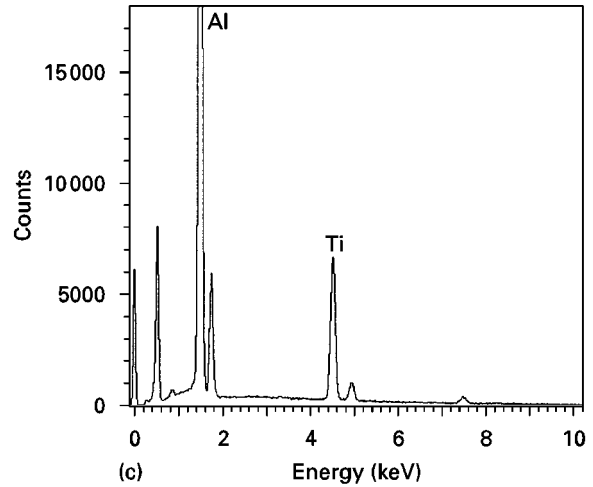
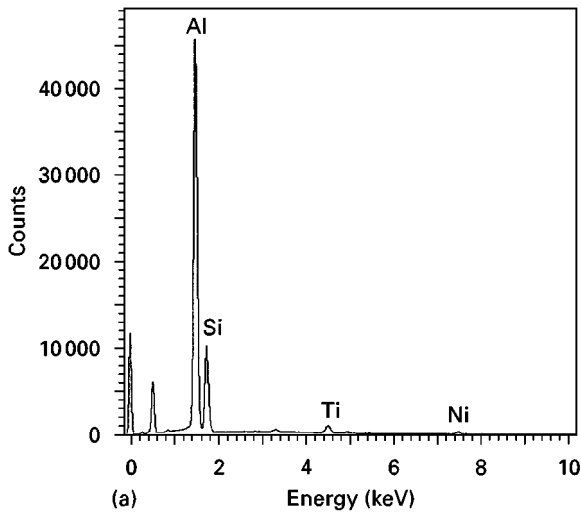
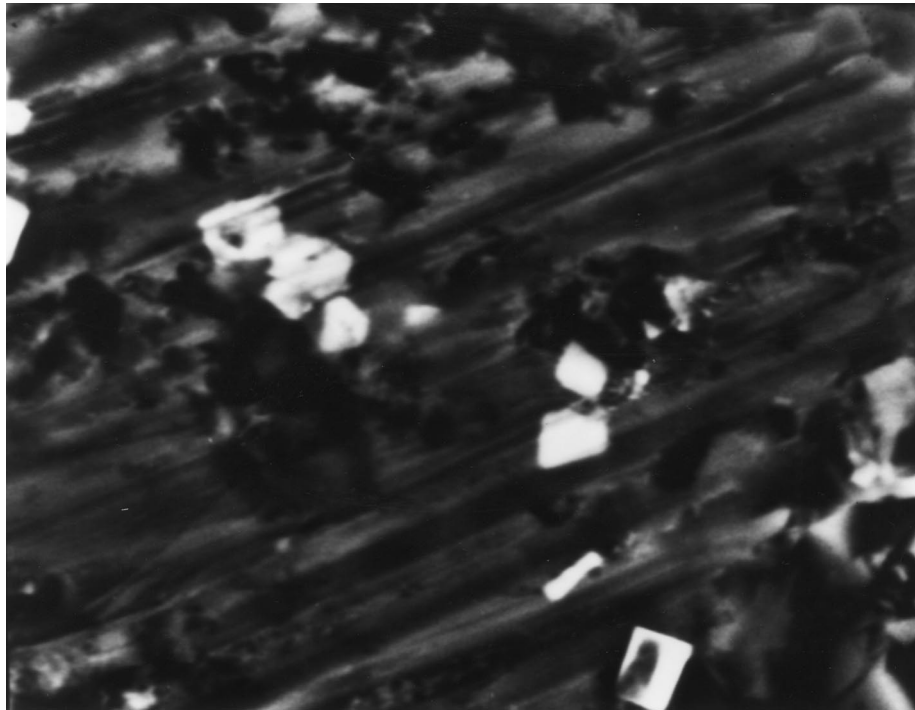


Figure 9 Back-scattered electron micrograph of sample CGB heated at 1400 °C/96 h and EDX spectra of (a) dark and (b) and (c) light areas.

by EDX (Fig. 9c). This crystalline phase was not detected by X-ray powder diffraction, which indicates a very small amount of this phase in the sample.

### 3.4. Optical properties

Diffuse reflectance spectra of samples C and D, for both series, fired at 1400 °C are displayed in Fig. 10. As can be seen, the spectra of the final samples are quite similar independently of the method of preparation. As was previously discussed, the spectra fit with that corresponding to the spinel  $\text{NiAl}_2\text{O}_4$ . The assignment of bands to electronic transitions was previously discussed by us in a recent paper [5].

Some consideration with respect to the possibility that  $\text{Ni}^{+2}$  introduced into mullite as a solid solution, as shown by EDX spectroscopy in Figs 8a and 9a, can influence the observed spectra, mainly associated with the spinel  $\text{NiAl}_2\text{O}_4$ , can be worthwhile. Although,

are formed by a matrix of doped-mullite solid solution in which  $\text{NiAl}_2\text{O}_4$  spinel particles are included. For CGB specimens (Fig. 9a and b), however, particles with compositions close to  $\text{Al}_2\text{TiO}_5$  are also detected

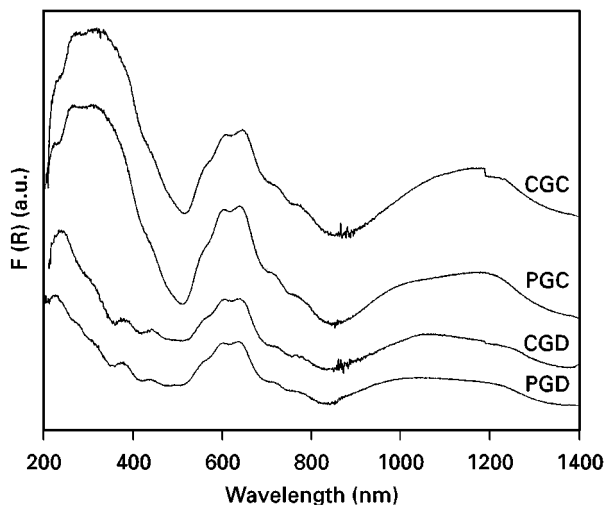


Figure 10 UV-Vis spectra of samples heated at 1400°C/96 h.

obviously, some  $\text{Ni}^{+2}$  is incorporated into the mullite matrix, because it will occupy preferentially octahedral positions, no large changes in band position, i.e. in energy, and intensity will be produced.

#### 4. Conclusion

The crystallization pathway to  $\text{NiAl}_2\text{O}_4$  spinel-mullite composites, obtained from precursors prepared either from polymeric and colloidal sol-gel techniques and subsequently non-isothermally treated, was followed. Differences in precursor chemistry of both types of precursor gel could explain changes in the reaction sequence. Thus, polymeric gels crystallized Al-Si spinel from the amorphous late in the temperature range between 850 and 1000°C,  $\text{NiAl}_2\text{O}_4$  spinel occurred as a secondary phase at slightly higher temperatures than Al-Si spinel, whereas in colloidal gel,  $\gamma\text{-Al}_2\text{O}_3$  and  $\text{NiAl}_2\text{O}_4$  crystalline phases appeared at 750°C. Mullite formation also took place at lower temperatures for PG than for CG specimens. The final set of phases in both series was quite similar. However, for CG-substituted gels, small amounts of secondary phases still remained for specimens after long annealing at 1400°C.

Differences in microstructure were only found for the larger particle size for the mullite matrix in CG

samples. Optical properties of both series of final specimens were also quite similar.

#### References

1. M. G. M. UISMAL, H. TSUNATORI and Z. NAKAI, *J. Am. Ceram. Soc.* **73** (1990) 537.
2. Q. M. YUAN, J. Q. TAN, J. Y. SHEN, X. H. ZHU and Z. F. YANG, *ibid.* **69** (1986) 268.
3. M. SALES, C. VALENTÍN and J. ALARCÓN, *J. Sol-Gel Sci. Technol.* **8** (1997) 871.
4. M. SALES and J. ALARCÓN, *Bol. Soc. Esp. Ceram. Vidr.* **34** (1995) 81.
5. M. SALES, C. VALENTÍN and J. ALARCÓN, *J. Am. Ceram. Soc.* **80** (1997) 1798.
6. M. SALES and J. ALARCÓN, *J. Eur. Ceram. Soc.* **16** (1996) 781.
7. J. A. PASK and A. P. TOMSI, *J. Am. Ceram. Soc.* **74** (1991) 2367.
8. D. W. HOFFMAN, R. ROY and S. KOMARNENI, *ibid.* **67** (1984) 468.
9. J. C. HULING and G. L. MESSING, *J. Am. Ceram. Soc.* **74** [10] (1991) 2374.
10. W. E. CAMERON, *Am. Mineral.* **62** (1977) 747.
11. B. E. YOLDAS, *Am. Ceram. Soc. Soc. Bull.* **54** (1975) 289.
12. B. FEGLEY and E. A. BARRINGER, in "Materials Research Society, Symposia Proceedings", Vol. 32, edited by C. J. Brinker, D. E. Clark and D. R. Ulrich (Elsevier Science, Amsterdam 1984) p. 187.
13. M. NOGAMI, S. OGAWA and K. NAGASAKA, *J. Mater. Sci.* **24** (1989) 4339.
14. F. PANCAZI, J. PHALIPPOU, F. SORRENTINO and J. ZARZYCKI, *J. Non-Cryst. Solids* **63** (1984) 81.
15. H. W. VAN DER MAREL and H. BEUTELSPACHER, in "Atlas of Infrared Spectroscopy of Clay minerals and their Admixtures" (Elsevier Science, Amsterdam, 1976) pp. 194, 275.
16. M. SALES and J. ALARCÓN, private communication.
17. W. WEI and J. W. HALLORAN, *J. Am. Ceram. Soc.* **71** (1988) 166.
18. S. SUNDARESAN and I. A. AKSAY, **74** (1991) 2388.
19. J. C. HULING and G. L. MESSING, in "Ceramic Transactions", Vol. 6, "Mullite and Mullite Matrix Composites", edited by S. Somiya, R. F. Davis and J. A. Pask (American Ceramic Society, Westerville, OH, 1990) p. 221.
20. D. X. LI and W. J. THOMSON, *J. Am. Ceram. Soc.* **74** (1991) 2382.
21. *Idem*, **73** (1990) 964.
22. W. WEI and J. W. HALLORAN, *J. Am. Ceram. Soc.* **71** (1988) 581.
23. W. G. FAHRENHOLTZ, D. M. SMITH and J. CESARANO III, *ibid.* **76** (1993) 433.
24. M. MIZUNO, *ibid.* **72** (1989) 377.

Received 3 February 1997

and accepted 15 May 1998